Science of the Total Environment 872 (2023) 162078

Contents lists available at ScienceDirect

Science of the Total Environment

journal homepage: www.elsevier.com/locate/scitotenv

Can online particle counters and electrochemical sensors distinguish normal periodic and aperiodic drinking water quality fluctuations from contamination?

Markus Koppanen [a,*], Tero Kesti [b], Jukka Rintala [a], Marja Palmroth [a]

[a] Faculty of Engineering and Natural Sciences, Tampere University, P.O. Box 541, FI-33101, Tampere, Finland
[b] Uponor Corporation, Kaskimäenkatu 2, FI-33900 Tampere, Finland

HIGHLIGHTS

- Periodicity in water consumption and water quality was studied.
- A flow-imaging particle counter classified particles by machine learning.
- Contamination event-specific particles are not detected in normal conditions.
- Selection of suitable particle channels is an alternative to dynamic baseline.
- Characteristics of artificial contamination vary from those of aperiodic events.

GRAPHICAL ABSTRACT

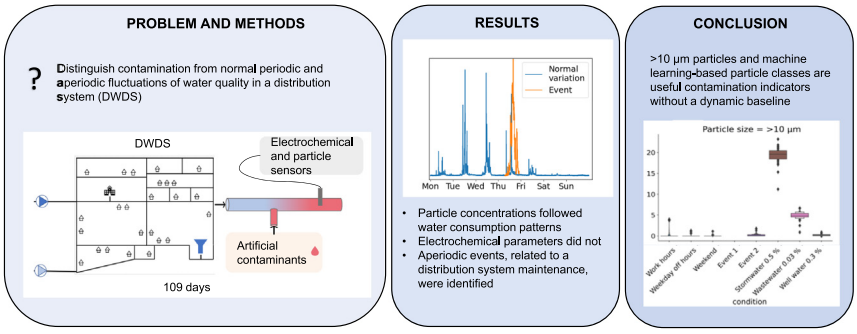

ARTICLE INFO

Editor: Damià Barceló

Keywords:
Distribution system
Early warning
Event detection
Flow-imaging
Hydraulic disturbance
Monitoring

ABSTRACT

Early warning systems monitoring the quality of drinking water need to distinguish between normal quality fluctuations and those caused by contaminants. Thus, to decrease the number of false positive events, normal water quality fluctuations, whether periodic or aperiodic, need to be characterized. For this, we used a novel flow-imaging particle counter, a light-scattering particle counter, and electrochemical sensors to monitor the drinking water quality of a pressure zone in a building complex for 109 days. Data were analyzed to determine the feasibility of the sensors and particle counters to distinguish periodic and aperiodic fluctuations from real-life contaminants. The concentrations of particles smaller than 10 µm and N, Small, Large, and B particles showed sudden changes recurring daily, likely due to the flow rate changes in the building complex. Conversely, the concentrations of larger than 10 µm particles and C particles, in addition to the responses of electrochemical sensors, remained in their low typical values despite flow rate changes. The aperiodic events, likely resulting from an abnormally high flow rate in the water mains due to maintenance, were detected using particle counters and electrochemical sensors. This study provides insights into choosing water quality sensors by showing that machine learning-based particle classes, such as B, C, F, and particles larger than 10 µm are promising in distinguishing contamination from aperiodic and periodic fluctuations while the use of other particle classes and electrochemical sensors may require dynamic baseline to decrease false positive events in an early warning system.

1. Introduction

Drinking water is essential for public health, and water quality and safety are ensured by a high-quality raw water source, efficient treatment processes, and the hydraulic integrity of drinking water distribution

* Corresponding author.
E-mail address: markus.koppanen@tuni.fi (M. Koppanen).

http://dx.doi.org/10.1016/j.scitotenv.2023.162078
Received 22 November 2022; Received in revised form 2 February 2023; Accepted 3 February 2023
Available online 9 February 2023

systems (DWDSs). Even though treatment processes generally produce water that meets national and international aesthetic, health-based and other quality criteria, the quality of drinking water may be compromised in DWDSs for several reasons. These reasons include failures in the physical integrity of DWDSs (e.g., a pipe break that causes an external contaminant intrusion), failures in the hydraulic integrity of DWDS (e.g., inability to maintain pressure and flow rate during maintenance period) (Besner et al., 2011), and the fact that DWDSs work as physical, chemical and biological reactors causing water quality to deteriorate during the transport phase from a drinking water treatment plant (DWTP) to customer taps (Chen et al., 2020; Fish et al., 2017; Liu et al., 2017).

To detect compromised drinking water quality in real time, an early warning system (EWS) integrated with an event detection system (EDS) can be established by utilizing online monitoring technologies and event detection algorithms instead of laborious, infrequent, and time-lagged grab sample analyses. Online water quality monitoring technologies commonly used in the routine monitoring of DWDSs and considered suitable for EWS include conventional sensors, such as conductivity, oxidation-reduction potential (ORP), chlorine concentration, pH, and turbidity (Dejus et al., 2018; Liu et al., 2014b; Storey et al., 2011). For instance, turbidity is a sum parameter for suspended particles, but it cannot characterize suspended solids to gain knowledge about the origin and behavior of the particles (Pronk et al., 2007), which may be beneficial for contamination detection due to potential water quality compromising scenarios involving particles, either chemical precipitates, microorganisms or their aggregates. More advanced methods have emerged in drinking water contamination studies to address the shortcomings of conventional sensor technologies, including spectroscopy (especially fluorescence) (Sorensen et al., 2018a, 2018b; Stedmon et al., 2011) and optical counting technologies such as flow cytometry (Besmer et al., 2017; Favere et al., 2020) and particle counting (Ikonen et al., 2013, 2017). Flow cytometry and a state-of-art application of particle counting, flow-imaging, are capable of high-frequency monitoring of suspended particles and they not only measure the number and size distribution of particles but also give an indication of microbial presence within these particles through either selective staining (flow cytometry) (Safford and Bischel, 2019) or particle morphology (flow-imaging) (Højris et al., 2016, 2018). Flow-imaging based on the machine learning analysis of images of particles is likely to be more robust and requires less maintenance than flow cytometry (Højris et al., 2016; Koppanen et al., 2022).

Continuous monitoring of water quality with different sensors can capture the short-term water quality fluctuations of a DWDS depending on the sensor. These fluctuations can be divided into periodic patterns, such as daily patterns that recur daily, and aperiodic events such as discoloration events, which refer to occasional events in which mobilized particle material on pipes leads to visible water discoloration. Previously, daily quality patterns associated with daily hydraulic changes (especially flow rate) were observed for several water quality sensors, including particle counters (Prest et al., 2021; Vreeburg et al., 2008), turbidity (Mounce et al., 2015; Sunny et al., 2020), conductivity, chlorine concentration and pH (Aisopou et al., 2012). However, these studies did not determine the range and distribution of periodic patterns, even though the processes of DWDSs are known to be stochastic by nature, nor did they compare the sensor responses to each other, such as particle characteristics and chemical parameters. Aperiodic events, such as discoloration events, are also typically related to hydraulic changes in flow rate, as a disturbance in hydraulic integrity by operational hydraulic changes may lead to exceptionally high flow velocities (shear stress) mobilizing an atypical proportion of accumulated particle material. Although discoloration events have been captured using turbidity sensors and particle counters and characterized reasonably well (Husband and Boxall, 2016; Mounce et al., 2015; Sunny et al., 2020), there are few studies of aperiodic events in which visible changes are not detected compared with discoloration events. It has been shown that water quality fluctuations, whether periodic or aperiodic, make it difficult to distinguish actual contamination events from these quality fluctuations (Housh and Ohar, 2017; Koppanen et al., 2022; McKenna et al., 2013). Thus, creating a dynamic baseline has been suggested (Favere et al., 2021), such as combining a hydraulic and water quality model with EDS (Housh and Ohar, 2017; Oliker and Ostfeld, 2015) in addition to monitoring parameters that do not respond to normal water quality fluctuations (Koppanen et al., 2022). Real-time hydraulic and water quality modeling is usually not available due to the insufficient availability of data, aside from the fact that water quality fluctuations are neglected in signal-processing based EDS studies (Housh and Ohar, 2017). Therefore, it is important to continue developing signal-processing-based EDS by studying the characteristics of water quality fluctuations. In addition, drinking water contamination studies typically rely on artificially produced normal water quality fluctuations (Housh and Ohar, 2017) or on setups that attenuate these fluctuations (e.g., a large tank between the distribution system and sensors) (Dejus et al., 2018; Ikonen et al., 2017). Thus, it is important to be able to compare periodic, aperiodic and contaminant fluctuations. To the best of our knowledge, no studies have reported periodic and aperiodic water quality fluctuations and fluctuations caused by actual contaminants using the same measurement setup.

The objective of the present study was to assess the feasibility of different online electrochemical sensors and particle counters to distinguish drinking water contamination from its periodic quality patterns and aperiodic events occurring in DWDS. For this purpose, the characteristics of periodic water quality patterns and aperiodic events were determined in the studied building complex in addition to the responses of simulated contamination tests. The study was performed using a set of electrochemical water quality sensors, a novel flow-imaging particle counter, and a more typical light-scattering particle counter to monitor drinking water quality for over 15 weeks.

2. Materials and methods

2.1. The study area and its monitoring

The study area was the pressure zone of a DWDS in a suburb with approximately 25,000 inhabitants including a university campus (10,000 students and 2000 employers), a science park and a water tower in Tampere, Finland (Fig. 1). The study was conducted from June 3 to July 16 (43 days) and from September 22 to November 26 (66 days) in 2020. During that time, many people were working from home due to the COVID-19 restrictions. The pressure zone is typically pressurized through the primary pressure booster station, the water of which is acquired from Lake Roine and treated in the primary DWTP with a capacity of 50,000 m^3/d. Occasionally, due to the maintenance shutdowns of the primary DWTP, the secondary DWTP with the same capacity produces water for the pressure zone from Lake Näsijärvi and the water is pressurized in the secondary pressure booster station.

The water flow rate in the study area was monitored in five locations: the primary DWTP, the primary and secondary pressure booster stations, a university building (representing a building complex), and a water tower. Hydraulic data were measured using the supervisory control and data acquisition system of the water utility (primary DWTP and pressure booster stations) or property maintenance (university building) at 60-min intervals.

Water quality was monitored in the university building and water tower. In the water tower, water quality was monitored in the inlet/outlet of the tower using a flow-imaging particle counter. In the university building, water quality was monitored with a set of electrochemical sensors (later referred to as the sensors) and flow-imaging and light-scattering particle counters installed in a test environment consisting of two lines. Drinking water continuously flowed through the lines, with a constant flow rate of 5500 mL per line and a retention time of 1 min from the tap to the sensors and particle counters. The test environment was also used for short-term contamination studies (Koppanen et al., 2022), but the present study utilized previously unpublished drinking water quality data measured outside the days of contaminant injections. The electrochemical water quality sensors (Endress + Hauser, Switzerland) used were ORP, free chlorine

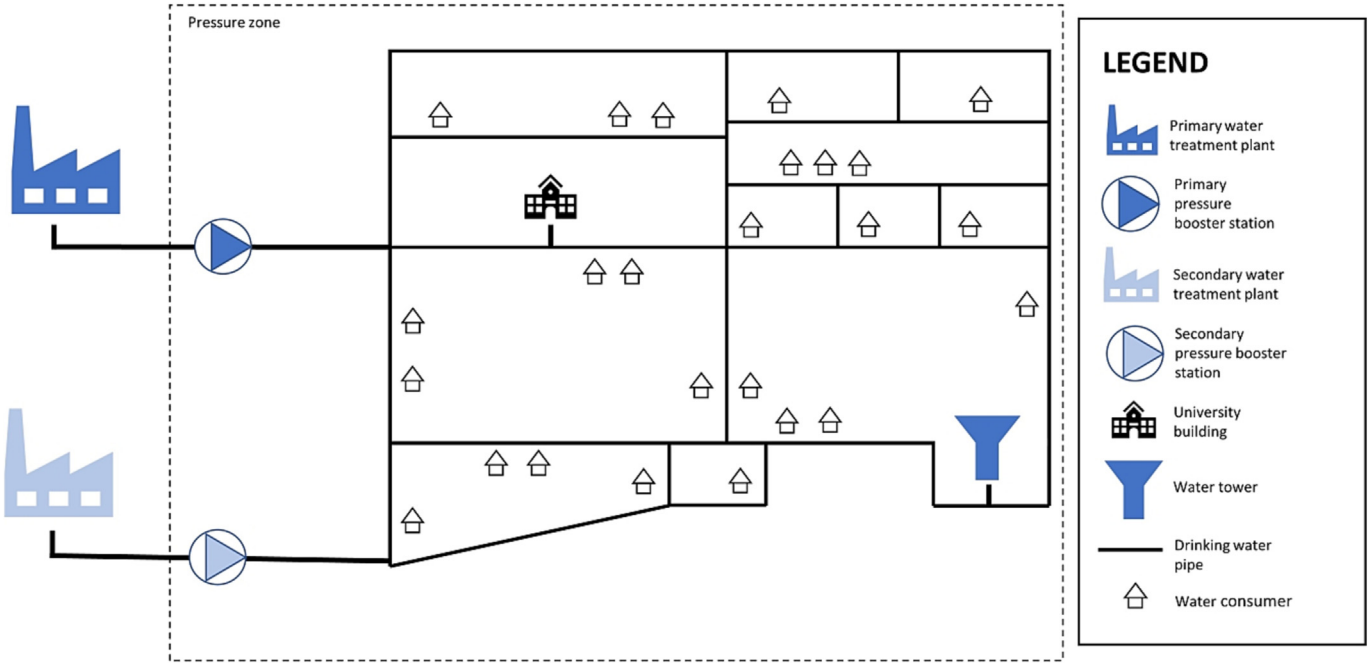

Fig. 1. A simplified representation of the study area including the monitoring locations. The pipe distance between the primary pressure booster station and the primary water treatment plant was approximately 1.2 km, with 100 % of the pipes being asbestos cement. The pipe distance between the primary pressure booster station and the university building was approximately 1.4 km, with 70 % of the pipes being ductile iron and 30 % were asbestos cement. The pipe distance between the university building and the water tower was approximately 2.3 km, with 100 % pipes of the pipes being ductile iron.

concentration, conductivity, and pH. The flow-imaging particle counter (a development version of the Qumo water quality monitoring station, Uponor Corporation, Finland) was a holographic microscopy-based online particle counter that uses machine-learning methods to determine the following six particle classes: N, B, C, F, Small, and Large. The N particle class depicts the total concentration of particles. The B, C, and F particle classes were based on a hybrid machine learning model that combined several deep neural networks, trained previously with stormwater contamination data not included in this work (Uponor R&D). In the B particle class, particles are typically larger than 3 μm, irregularly shaped, and observed in the mobilized particle material of drinking water pipe walls. The C particle class consists of larger than 3 μm particles that are found in wastewater and stormwater. The F particle class consists of elongated fiber-like particles. The Small and Large particle classes were related to size with Small indicating particles <1 μm and Large indicating particles larger than 2 μm. The light-scattering particle counter (PAMAS Partikelmess- und Analysesysteme GmbH, Germany) had the following eight channels for different particle sizes: 0.5–0.7, 0.7–1, 1–2, 2–5, 5–10, 10–15, 15–20, and > 20 μm.

2.2. Determination of fluctuations and periodic patterns for water flow rate and quality

Water flow rate and quality data were preprocessed for further data analysis by merging the data from both study periods into one combined dataset and, in the case of water quality data, by manually or automatically removing the sensor/particle counter and equipment maintenance periods and other arbitrary measurement artifacts. The arbitrary measurement artifacts were identified by going through the data week by week and comparing the days of the week (Monday–Sunday) with each other between the weeks, or by utilizing the self-diagnostic features of the flow-imaging particle counter and removing them from the combined dataset. The automatic removal of measurement artifacts was implemented for the light-scattering particle counter channel of 0.5–0.7 μm as it occasionally involved periods of 5-min artifacts (values up to 800,000 particles/mL) repeating every 5 min probably due to air bubbles entering the measurement channel. These short measurement artifacts were removed using a moving minimum with a window of 10 min using the Rolling.min rolling window function in the Python (v. 3.8.3) library Pandas (v. 1.05).

The flow rate and water quality sensor/channel fluctuations were analyzed statistically by determining two parameters that describe close to the median and extreme fluctuations. The presence of close-to-median fluctuations was assessed by calculating the relative dispersion of the flow rate and sensor/channel responses, that is, the quartile coefficient of dispersion in which the differences of the 75th and 25 percentiles were divided by the sum of the 75th and 25th percentiles (Bonett, 2006). The resulting ratios are unitless, thus making the responses of flow rate and different sensors/channels comparable with each other. The higher the dispersion ratio, the higher the dispersion of the response. The presence of extreme fluctuations and their frequency in the dataset were assessed using the ratio of extreme percentile values. The ratio of the 90th and 99.5th percentiles–90/99.5 ratio–was calculated, similar to the study of Vreeburg et al. (2008), to estimate the sudden extremely high values of the responses of the flow rate and all the sensors/channels. The 90/99.5 ratio decreases when the difference between the 90th and 99.5th percentiles increases, indicating a higher variation in high values. The ratio of the 0.5th and 10th percentiles–0.5/10 ratio–was calculated to estimate the number and density of sudden extremely low values for the following parameters: flow rate, free chlorine concentration, and ORP. Similar to the 90/99.5 ratio, the 0.5/10 ratio decreases when the difference between the 0.5th and 10th percentiles increases, indicating higher variation in low values.

The patterns were determined using weekday and weekend scales to study how the time scale affected the periodicity and variation of the responses, and how the water flow rate was compared with the responses of water quality sensors/channels. The dataset was divided into two groups, namely, weekdays (Monday–Friday) and weekends (Saturday–Sunday), which were visualized, and their hourly distributions (25th, 50th, and 75th percentiles) were calculated and visualized. To create a typical weekly pattern, each combined dataset was divided into seven subsets, each covering one day. These seven subsets, for example, Mondays, were divided into 24 subsets of 1 h. A pattern for each day of the week was calculated by determining a median response (50th percentile) for these 60-min subsets. To

obtain comprehensive insights into the distribution of these subsets and to assess the characteristics of the periodicity of the data, the 25th and 75th percentiles, which constituted the middle 50 % of sensor responses, were calculated for each 60-min subset. This processing of 1-h subsets standardized different measuring intervals between the sensors without the need for actual resampling.

2.3. Effects of aperiodic and contamination events on water quality

The water quality was monitored, and the dataset was analyzed during two aperiodic events related to the shutdown of the primary DWTP and the usage of the secondary water source to produce water for the pressure zone. Water from the secondary DWTP was conveyed to the area through a secondary pressure booster station. The use of a secondary booster station led to hydraulic changes in the studied DWDS. The water utility informs the residents of possible temporary drinking water discoloration when the secondary booster station is used. In the first event (Event 1), a pipe leak was observed in the proximity of the raw water pump site on June 18, while the second event (Event 2) was related to the maintenance shutdown of the primary DWTP due to the renovation of the technical processes of the plant on October 29.

The artificial contaminants were studied in a test environment with two lines; one line was used to examine drinking water quality, as presented above, while contaminants were injected into the other line. Both lines contained the electrochemical sensors and particle counters, as described in Section 2.1. The contaminant injections studied were stormwater 0.5 % (v/v) (undiluted characteristics: pH = 7.1, ORP = 356 mV, conductivity = 120 μS/cm, turbidity = 68 NTU, total suspended solids = 18 mg/L), wastewater 0.03 % (v/v) (undiluted characteristics: pH = 7.6, ORP = 118 mV, conductivity = 855 μS/cm, turbidity = 140 NTU, total suspended solids = 168 mg/L), and well water 0.3 % (v/v) (undiluted characteristics: pH = 6.9, ORP = 122 mV, conductivity = 632 μS/cm, turbidity = 122 NTU, total suspended solids = 24 mg/L). The data of each sensor/channel response during contaminant injections (each lasting for approximately 30 min) were compared to periodic and aperiodic water quality fluctuations determined based on the 109 days study period.

2.4. Water quality parameter distributions and false positive rate calculation

The measured water quality sensor/channel distributions under normal operation conditions, Events 1 and 2, stormwater, wastewater, and well water injections were visualized as a letter-value box representation (Hofmann et al., 2017) created using the seaborn visualization library (Waskom, 2021).

To estimate the reliability by which the artificial contaminations could be distinguished from normal periodic fluctuations and Events 1 and 2, a false positive rate (FPR) was calculated for each combination of contaminant concentration and response of the sensor/channel based on the expected response direction. $FPR_{increase}$ or $FPR_{decrease}$ was calculated based on whether the sensor/channel response was likely to increase or decrease due to a contaminant injection, respectively, as follows:

$$FPR_{increase} = \frac{N_{c_{ref} > c_{cont}}}{N}, \quad (1)$$

$$FPR_{decrease} = \frac{N_{c_{ref} < c_{cont}}}{N}, \quad (2)$$

where the number of data points (N) measured during the reference period (normal operation, Events 1, or 2), under the condition that the measured concentration c_{ref} exceeds or falls below the mean concentration c_{cont} during the contamination injection, is divided by the total number of data points N in the reference period. Therefore, FPR shows the probability that either normal quality fluctuations or a discoloration-like event similar to Event 2 would have caused a greater response than artificial contamination. By using the maximum acceptable FPR of 0.5 %, the most suitable water quality sensors/channels for detecting contaminants can be selected.

3. Results and discussion

To determine the normal periodic pattern characteristics (i.e., periodicity, distribution and range of fluctuations in sensor/channel responses), water quality and flow rate patterns (Fig. 2) were studied. The patterns were derived from 15 weeks of flow rate and water quality data (79 days between Monday and Friday and 30 days between Saturday and Sunday) in the studied pressure zone. The monitoring period included two aperiodic events caused by hydraulic disturbances that altered the responses of electrochemical sensors and particle counters. To distinguish the sensor/channel responses caused by contamination from aperiodic and periodic water quality fluctuations, sensor/channel responses to all three cases were analyzed statistically.

3.1. Short-term periodic fluctuations in normal conditions

The periodic flow rate patterns of the pressure booster station and the university building were analyzed to interpret the flow rate characteristics leading to periodic water quality patterns and to provide a more comprehensive understanding of the pressure zone (Fig. 1). The changes in water quality measured by electrochemical sensors and particle counters in the university building were analyzed to study the characteristics of periodic fluctuations.

3.1.1. Water flow rate

The outflow of the primary booster station showed a double peak periodic pattern (Fig. 2B), in which flow rate was the highest (typically 300 m^3/h) at around 12:00 and again at around 22:00. The filling of the water tower during the night (00:00–06:00) could be observed as a relatively high flow rate in the periodic pattern. In general, the water flow rate pattern varied more on weekdays than on weekends. On weekdays, the 0.5/10 ratio of the flow rate was considerably lower, and the quartile coefficient of the dispersion was higher than on weekends (Table 1), indicating a higher variation in extremely low values (sudden flow rate spikes close to zero) and in the middle 50 % values in the primary booster station. The shape of the flow rate pattern in the university building was different from that of the primary booster station, peaking typically at 1.3–2.0 m^3/h at around 12:00 on weekdays (Fig. 2A). At night (18:00–07:00) and on weekends, the flow rate was typically 0.7–0.8 m^3/h, to which the consumption caused by the test environment (0.72 m^3/h) contributed almost all. Based on the water flow patterns, the water quality monitored in the university building during nights and weekends represented the water quality of the DWDS. During daytime on weekdays, the water quality was also affected by the changes in water consumption in the distribution system (opening and closing of valves) of the university building. Thus, in the following, water quality fluctuations are compared, considering the differences in these two main periods.

3.1.2. Water quality

In the university building, the electrochemical sensors, including free chlorine concentration, ORP, conductivity, and pH, generally revealed periodic water quality patterns in their responses when the middle 50 % was determined (dashed and solid line in Figs. 2C–2F), although the middle 50 % and variation in the extreme values were relatively low, especially for ORP, conductivity, and pH (Table 1). The daily periodicity was observed on weekdays, for example, as an increase in the response of free chlorine concentration and ORP between 08:00 and 16:00, followed by a decrease until 08:00 the next morning. On weekends, the increase in responses was observed between 13:00 and 18:00, and the largest decrease was at around 12:00. The pattern of pH was inversely proportional to those of the free chlorine concentration and ORP. The response of conductivity was 1–2 μS/cm higher during work hours (8:00–18:00) than outside of them.

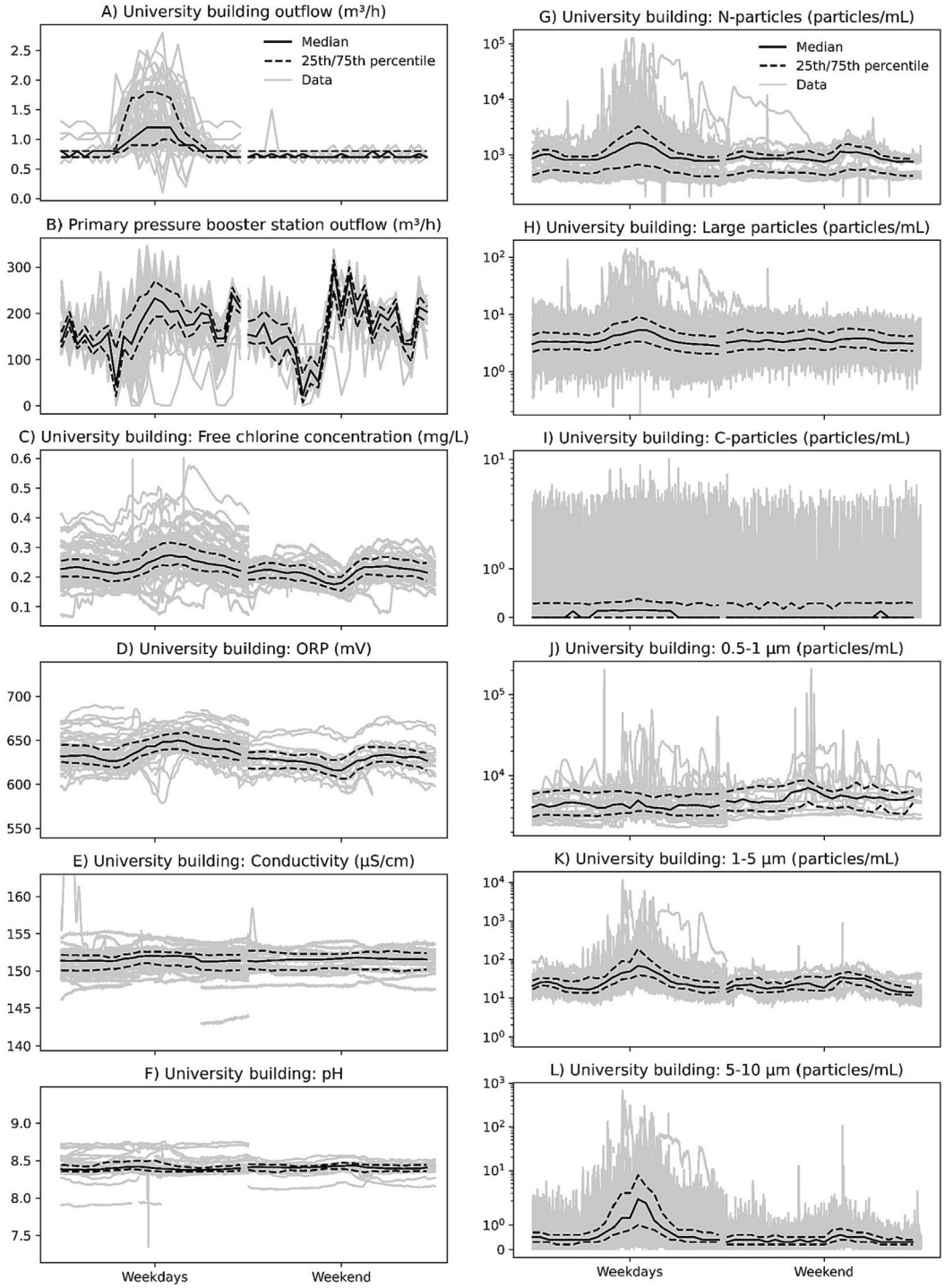

Fig. 2. The flow rate (university building, primary pressure booster station), electrochemical sensor responses measured in the university building (free chlorine concentration, oxidation-reduction potential (ORP), conductivity, pH), responses of the flow-imaging particle counter channels (N, Large, C), and light-scattering particle counter channels (0.5–1 µm, 1–5 µm, 5–20 µm) measured in the university building shown as weekday and weekend patterns. All data are depicted in gray. The dashed line (–) represents the 25th and 75th percentiles, and the solid line (−) represents the 50th percentile of the data. The weekdays and weekend labels are aligned with midday (12:00).

Using both studied particle counters, the concentrations of the particles in each measurement channel showed periodic responses with the highest fluctuations on weekdays (Table 1), centering around 12:00. However, the particle concentrations also fluctuated to some extent during nighttime and weekends when the flow rate in the university building was close to constant (Fig. 2G–L), suggesting changes in the water quality of the water mains of the DWDS. In addition to the patterns of the particle size classes of the light-scattering particle counter between 1 and 10 µm, the patterns of particle classes N (similar pattern to that of Small class; see Fig. S1D), Small, Large, C, and B (similar pattern to that of Large class; see Fig. S1E) of the flow-imaging particle counter seemed to follow the flow rate pattern of the university building (Fig. 2A). The following shows the similarity of the particle class and flow rate patterns: sudden extreme spikes occurred in the concentrations of N, Small, Large, B classes and 1–10 µm size classes between 09:00 and 16:00 on weekdays when the flow rate was twofold compared with weekends when such particle spikes were not observed as

Table 1
The ratio between the 90th and 99.5th percentiles (the ratio between the 0.5th and 10th percentiles in brackets) and the quartile coefficient of dispersion in different flow rates and water quality sensor responses. The lower the 90/99.5 ratio or 0.5/10 ratio, the higher the variation in extremely high or low values, respectively. The quartile coefficient of dispersion shows a relative statistical dispersion based on the 25th and 75th percentiles (lower values indicate lower relative dispersions).

	90/99.5 ratio (0.5/10 ratio for the flow rate, free chlorine concentration, oxidation-reduction potential)		Quartile coefficient of dispersion (75th percentile - 25th percentile) / (75th percentile + 25th percentile)	
	Weekday	Weekend	Weekday	Weekend
Flow rate				
University building inflow	0.76 (0.625)	1 (1)	0.31	0.07
Primary pressure booster station	0.83 (0.01)	0.93 (0.79)	0.26	0.08
Electrochemical sensors				
Free chlorine concentration	0.65 (0.62)	0.86 (0.87)	0.12	0.14
Oxidation-reduction potential	0.98 (0.98)	0.99 (0.99)	0.013	0.016
Conductivity	0.990	0.994	0.005	0.007
pH	0.996	0.996	0.007	0.005
Flow-imaging particle counter				
N	0.065	0.89	0.57	0.34
Small	0.22	0.74	0.43	0.27
Large	0.11	0.70	0.41	0.30
B	0.05	0.70	0.86	0.84
C	0.21	0.15	1	1
Light-scattering particle counter				
0.5–0.7 μm	0.34	0.69	0.32	0.16
0.7–1 μm	0.11	0.47	0.39	0.27
1–2 μm	0.04	0.83	0.50	0.21
2–5 μm	0.03	0.70	0.53	0.40
5–10 μm	0.03	0.55	0.63	0.33
10–15 μm	0.06	0	Undefined	Undefined
15–20 μm	0	Undefined	Undefined	Undefined
>20 μm	0	0	Undefined	Undefined

Undefined = division by zero

often. The responses of the smallest size classes of 0.5–1 μm were different from those of the 1–10 μm size classes since they also showed spikes on weekends. The 90/99.5 ratio of the C particles was similar between weekdays and weekends (0.21 and 0.15, respectively), aside from its relatively low concentration (middle 50 %: 0–0.4 particles/mL) throughout the day, suggesting that the periodic flow rate of the primary pressure booster station or the university building did not alter the concentration of the C particles. The middle 50 % concentration of the F particles was even lower than that of the C particles, but it manifested spikes up to 300 particles/mL, centering at around 12:00 (Fig. S1H).

The findings of the present study suggest that among the studied online monitoring technologies, particle counters are better suited to monitor periodic water quality changes related to flow rate changes in DWDSs than electrochemical sensors. In particle counters, particles 1–10 μm and machine learning-based particle channels, including N, Small, Large, and B, seem to be the most feasible to follow periodic water quality fluctuations in normal DWDS conditions. In these normal operation conditions, equilibrium between the liquid (bulk water) and solid phases (suspended solids, pipe wall biofilm, and loose deposits) is sustained throughout the DWDS (Chen et al., 2020). This is referred to as the accumulation–mobilization process, in which the higher flow rate causes higher shear stress to the pipe walls, mobilizing the particle material that accumulated on the pipe walls during lower flow rates (Sunny et al., 2020). The periodic suspended solids are directly related to drinking water quality, since their presence may increase the risk of discoloration of water (Mounce et al., 2015; Sunny et al., 2020; Vreeburg et al., 2008). Moreover, suspended solids provide a surface area for the attachment of microorganisms and act as a source of nutrients to them, possibly increasing their growth potential in the DWDS (Liu et al., 2014a). The results of the present study show, that even if the sudden extreme changes caused by the building complex flow rate mobilize the particles, they do not affect the responses of the electrochemical sensors (i.e., conductivity, free chlorine concentration, pH and ORP). This is because the electrochemical characteristics of drinking water typically depend on disinfection practices, as the amount and efficiency of chlorine in DWDS are controlled by water residence time, pH, and chlorine decay rate (Polycarpou et al., 2002) and the effect of the accumulation–mobilization process (i.e., sudden changes in these characteristics) has likely been very small. However, if the mobilized material is oxidized by chlorine, the concentration of chlorine and the responses of other electrochemical sensors may be more affected.

3.2. Hydraulic disturbances cause aperiodic fluctuations

The effects of hydraulic disturbances and water source changes caused by maintenance work on water quality as aperiodic fluctuations were studied on three occasions (referred to as Events 1A, 1B, and 2) in the university building and the water tower to illustrate the propagation of aperiodic fluctuations in the pressure zone. During these events, the secondary pressure booster station was used to pump water to the pressure zone, either up to a flow rate of 200 m^3/h (Event 1B, 2) or 120 m^3/h (Event 1A) (Fig. 3A and F). The primary DWTP and the primary pressure booster station stood idle in Events 1A and 2, while they operated simultaneously with the secondary pressure booster station in Event 1B.

During Events 1B and 2, considerable increases in the N particle concentration from the periodic fluctuations were detected in the university building. Event 2 was not detected in the water tower, since the water tower was filled during the night, and Event 2 occurred during the day when the water flowed out of the water tower (for details on the water tower control, see Section 3.1). In Event 1B, the N particle concentration increased 4 h after the initiation of the secondary pressure booster station and showed a broad spike between 23:00 and 11:00, peaking at 17000 particles/mL, in the university building and between 22:30 and 07:30, peaking at 11550 particles/mL in the water tower. After Event 1B, the N particle concentration in the water tower was up to 170 % higher than that of Event 1B for the next two days. This concentration decreased stepwise when the water from the DWDS flowed into the water tower everyday between 00:00 and 06:00, until it stabilized at around 1500 particles/mL (data not shown). Compared to Event 1B, Event 2 had up to a 365 % higher N-particle concentration during the period of 10:00–02:00, creating a broad spike in the university building. During Event 2, the light-scattering particle counter was operational, showing an increase in the response of all size channels except for the 15–20 μm and > 20 μm channels (Fig. S3). Unlike in events with a

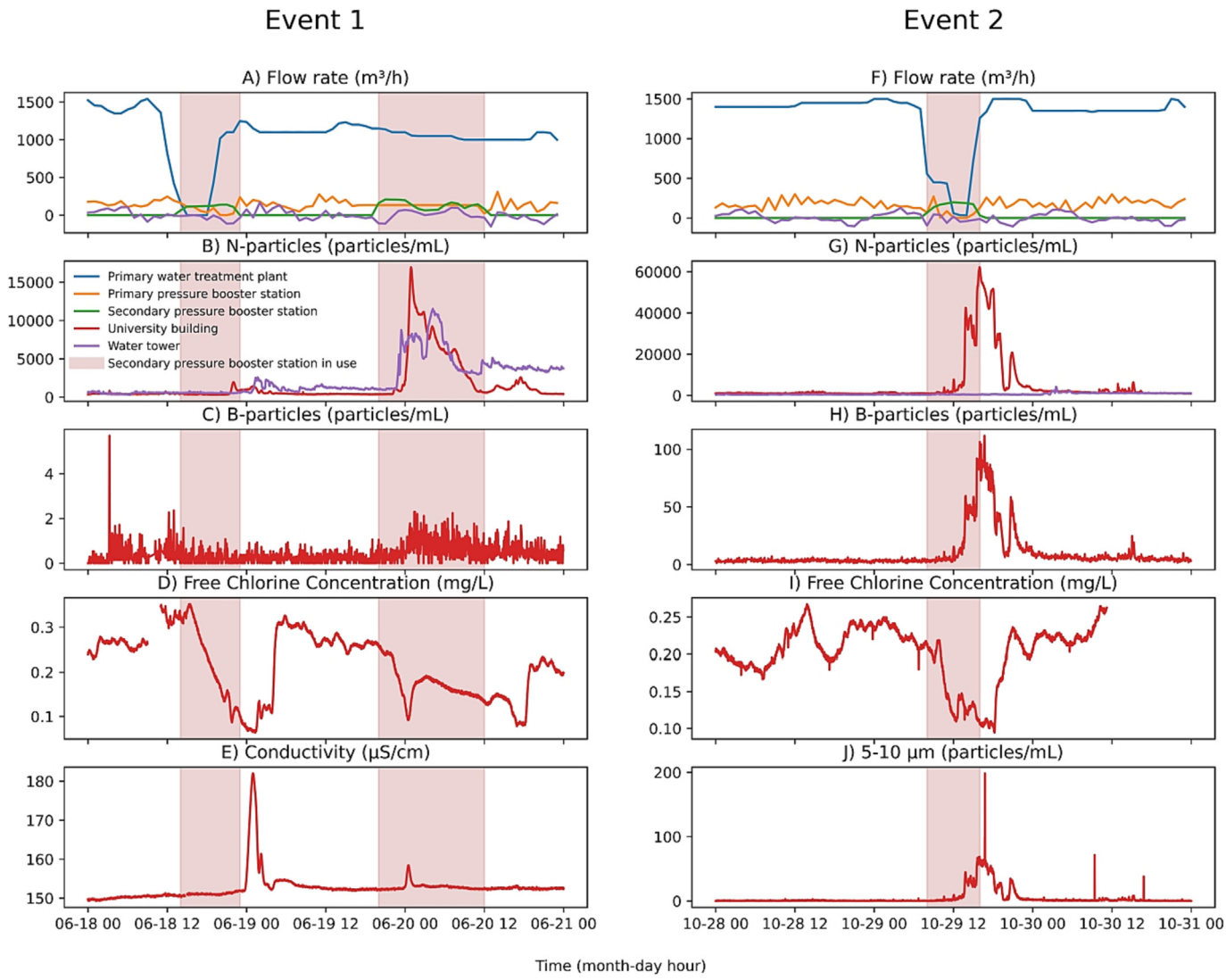

Fig. 3. Two captured aperiodic events illustrated by the flow rate of four monitoring locations (primary water treatment plant, pressure booster stations, university building, water tower), the selected channels of the flow-imaging particle counter (N, B), the light-scattering particle counter (5–10 µm), and the selected conventional sensors (free chlorine concentration, conductivity) in the university building and the water tower. The flow rate of the water tower has a positive sign when flow is conveyed into the tower and a negative sign when flow is conveyed out of the tower. Events were captured on June 18 (Event 1A), June 19–20 (Event 1B), and October 29 (Event 2).

higher flow rate in the secondary pressure booster (Event 1B and 2), in Event 1A, the N particle concentration increased from 350 particles/mL to 2000 particles/mL between 21:30 and 04:00, creating a series of broad spikes observed in the university building. In the water tower, the N particle concentration increased from 500 to 600 particles/mL to 2600 particles/mL during the period of 00:30–06:00. However, the N particle concentration remained at 1300–1500 particles/mL until Event 1B, since during that time, the particle counter measured the water leaving the tower. The concentrations of the B and F particles increased (100 particles/mL and 2 particles/mL, respectively) in Event 2, while these concentrations remained at their typical low level during Events 1A and 1B. The concentration of the C particles remained at its typical low level during all events even though an increase of 1–3 particles/mL was observed in Event 2 in the same period as the N particle increase.

The decrease in free chlorine concentration showed similarities between Event 1A and Event 2 in the university building. In Event 1A, the free chlorine concentration decreased to 0.06 mg/L in the university building 2.5 h later than the initiation of pumping from the secondary pressure booster station, and the concentration remained low for the next 14 h. Event 2 showed a decrease in the free chlorine concentration from 0.19–0.25 mg/L to 0.1 mg/L between 10:00 and 21:00 (11*h*). Compared with the 14-h and 11-h periods of the low free chlorine concentration in Event 1A and 2, respectively, Event 1B showed only a decrease in free chlorine concentration to 0.08 mg/L for 5 h, but the residence time was 2.5 h. The observed conductivity spikes, approximately an increase of 30 µS/cm for Event 1A and an increase of 5 µS/cm in Event 1B, could be related to the drinking water originating from the secondary DWTP since it had slightly a higher conductivity of water, 187 µS/cm on average, compared with the conductivity fluctuations of the primary DWTP measured in the university building (Fig. 2E).

The results from the studied events suggest that the responses of the particle counters, especially the channels related to a smaller particle size (N, Small, 0.5–10 µm) and conductivity, can be used to determine how the hydraulic disturbances and possible water source changes caused by the primary DWTP maintenance affect water quality and how long the quality changes last. It seems that the flow rate of the secondary pressure booster station caused increases in particle concentration, since Events 1B and 2, with a 67 % higher flow rate than 1A, showed considerably higher particle concentrations than Event 1A and periodic fluctuations. Recent independent observations of the water utility also support this, since the water utility personnel have noticed that the use of higher flow rates in the secondary booster station leads to discoloration in the pressure zone.

Conductivity, which can be an indicator of water origin, showed 3.5-h spikes in Events 1A and 1B, indicating that during these spikes, an abnormal amount of water originated from the secondary DWTP. However, in Event 1A, it took 10.5 h until the conductivity spike was observed after the initiation of the secondary booster station while it took only 3 h in Event 1B. Therefore, it can be speculated that the DWDS between the secondary booster station and the secondary DWTP probably contained mostly water from the primary DWTP prior to Event 1A, whereas prior to Event 1B, the DWDS between the secondary pressure booster station and the DWTP seemed to contain mostly water from the secondary DWTP, thus leading to a shorter residence time. In the literature, higher flow rates causing increased shear stress on pipe walls are interpreted as the primary cause of discoloration events, and water source changes are considered a possible contributing factor (Husband and Boxall, 2016).

Although the observed aperiodic events did not cause reported customer contacts or water epidemics and were predictable at some level to the water utility, the considerable increases in particle concentration lasted up to 12 h with the free chlorine concentration decreasing close to zero in the university building. In addition, in Event 1B, the water tower was filled with water containing a high particle concentration, which was distributed to customers the following day. For future research, it might be useful to study such predictable events with detailed microbial analyses, including pathogens and/or sensors that are able to distinguish microbial and nonmicrobial contaminants, since particle abundance does not confirm whether there are microbiological risks related to exposure to water.

3.3. Distinguishing contamination from periodic and aperiodic fluctuations using statistics

To detect real water contamination with online measurements, it is necessary to distinguish contamination from normal periodic and aperiodic water quality fluctuations. For this purpose, approximately 30 min contamination injections were performed in the second line of the test environment, and the responses were analyzed statistically to determine the contamination detection performance for flow-imaging and light-scattering particle counters channels, conductivity, and free chlorine concentration. The statistical plots in Fig. 4 condense the sensor/channel response variation in the three contamination injections compared with those in the periodic and aperiodic fluctuations (described in Sections 3.1 and 3.2). The FPR calculated in Tables S1 and S2 are complementary compared with the statistical plots to assess the separability of the contamination injections from periodic fluctuation and aperiodic events.

The responses to the injection of stormwater (0.5 % v/v) for all the size channels of the light-scattering particle counter overlapped little or not at all with those of either periodic fluctuation (weekdays and weekends) or aperiodic fluctuation (Event 2). The injection of wastewater (0.03 % v/v) overlapped with aperiodic fluctuations (Event 2) for all the size channels of the light-scattering particle counter, except for particles larger than 10 μm. Similarly, the responses of the flow-imaging particle counter channels N and Small to the injections of stormwater and wastewater overlapped with aperiodic event data, while the responses of the Large and C channels did not. The FPR values below 0.5 % were found for the 10–15 μm, 15–20 μm, Large, B, C, and F channels for periodic fluctuations (Table S1), and 10–15 μm, 15–20 μm, and Large channels for aperiodic event 2 (Table S2) in wastewater and stormwater contaminants. Well water, which consisted of a relatively high concentration of small particles and few large particles in contrast to stormwater and wastewater, overlapped little with the periodic fluctuations (only with C particles) and aperiodic event 2 overlapped with >2 μm, N, C, and F channels, resulting in below a FPR of 0.5 % for 0.5–0.7 μm, 0.7–1 μm, 1–2 μm, Small channels. In the electrochemical sensors, the decrease in free chlorine concentration due to the contaminant injections was approximately 0.1 mg/L, overlapping with periodic fluctuations and Event 1, resulting in a FPR of 55–82 %. Similarly, conductivity overlapped with periodic fluctuations, even though the conductivity response during stormwater 0.5 % (v/v) injection was considerably low (FPR = 5 %) in comparison with periodic fluctuations.

The present study shows that the differences between the studied contaminants (stormwater, wastewater, and well water) and periodic fluctuations were detected in all the channels of the light-scattering and flow-imaging particle counters. As noted in Section 3.1, extreme spikes around working hours were observed in the responses of the particle channels, except for the largest size classes of 10–20 μm and machine learning-based C particles, indicating their potential in contamination detection. If such extreme spikes are common due to sudden increases in flow rates as in the present study, it could be difficult to make a decision on what is large enough change in the sensor response to justify action. Prest et al. (2016) highlighted a major knowledge gap related to the degree of acceptable change in biological stability (microbial counts), which also translates to contamination detection, since the sensors used are typically not able to evaluate health risks caused by water contamination. McKenna et al. (2008) noted that 20 %–30 % of the changes between adjacent measurements derived from normal water quality fluctuations could make it challenging to classify an event as a true negative instead of a false positive in EDS. Thus, sensors/channels not responding to periodic water quality changes, especially to extreme spikes, should be favored in contamination detection. Drinking water studies advancing signal-processing-based EDSs consist of designing an event detection algorithm that can distinguish normal fluctuations from contamination (Dejus et al., 2017; Liu et al., 2016) rather than finding a sensor/channel that responds exclusively to possible contaminants. In the case of the present study, the electrochemical sensors and particle channels N, B, Small, Large, 1–10 μm responded to hydraulic changes (i.e., flow rate changes). For these channels, the use of real-time hydraulic modeling to implement a dynamic baseline for water quality may decrease the number of false positives, similarly to Housh and Ohar (2017, 2018). The contamination detection performance of different sensor/channel responses with and without a dynamic baseline could be compared in future studies.

The present study shows that the most suitable sensors/particle channels for distinguishing stormwater or wastewater contamination from aperiodic events are the flow-imaging particle counter channels C and F and the light-scattering particle counter channels >10 μm. Moreover, the B particles of the flow-imaging particle counter showed promising results since they were able to distinguish between Events 1B and 2 (Fig. 3C and 3H) and were the only channel/sensor capable of such maneuvers. Distinguishing well water contamination from aperiodic events proved to be difficult because well water contained mostly small particles and few large particles compared with stormwater and wastewater, which contained more larger particles. The aperiodic events shown in the present study are likely to be similar to discoloration events which have usually been shown to include particles with a size of 10 μm (Husband and Boxall, 2016), similar to the particle sizes present in the stormwater and wastewater. However, the present study challenges this assumption because it seems that there are also aperiodic events with a smaller dominating particle size, and which do not cause discoloration of water. In addition to the different water quality characteristics of the contaminants, the characteristics of the DWDS of the present study contained mostly particles smaller than 10 μm which were observed especially in the sudden changes during working hours (periodic patterns) and aperiodic events, but the water quality characteristics may differ among DWDSs and in different parts of a DWDS. Larger particles have been found further down DWDSs (Prest et al., 2021; Verberk et al., 2006). The university building in the present study was located only 2 km away from the DWTP, unlike in the study of Vreeburg et al. (2008) who found particles larger than 10 μm from a DWDS 40 km away from the DTWP. For future research, it may be productive to monitor periodic and aperiodic water quality patterns using particle counters in locations where particles larger than 10 μm are more common unlike in the present study. The machine learning-based particle classes of the flow-imaging particle counter were able to distinguish different events, but it should be noted that their performance relied heavily on training data. To achieve more suitable results for any DWDS, training data should cover data from multiple DWDSs, and algorithms could be trained again when enough data are gathered from the DWDS.

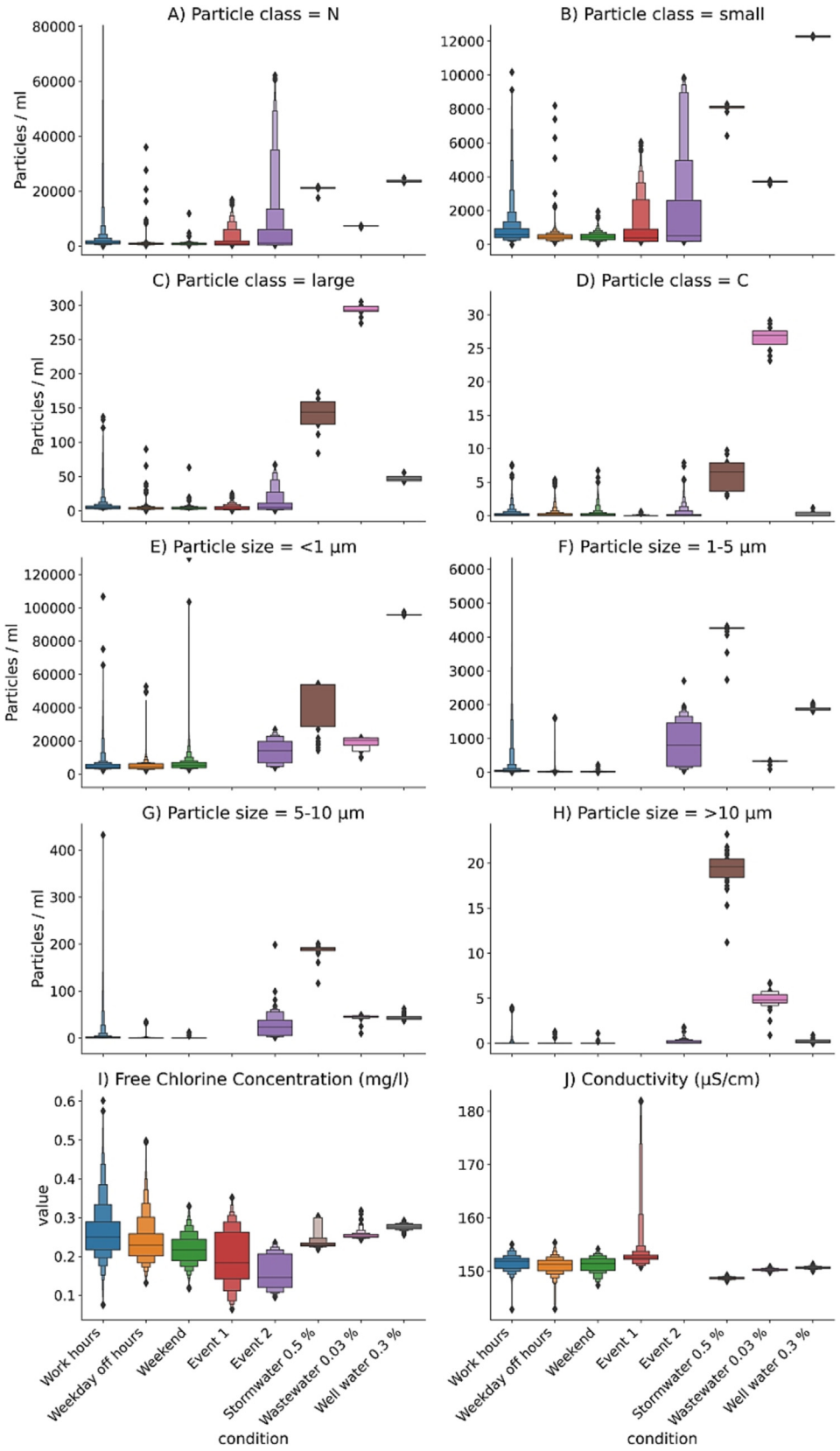

Fig. 4. Distribution of particle concentrations during weekday work hours, weekday off-hours, weekends, Event 1 and 2, and the injections of stormwater, wastewater and well water as classified by the light-scattering particle counter particle sizes (A–D), flow-imaging particle counter particle channels (E–H), free chlorine concentration (I), and conductivity (J). The distribution is shown as a letter-value box, in which the largest box represents the middle 50 % (25th, 50th, and 75th percentiles) and the next largest box represents half of the remaining data (37.5th and 87.5th percentiles), and so forth. Outliers are shown as single datapoints. The conditions are weekday working hours (8:00–18:00), weekday off-hours, weekend, Event 1 (from 15:00 on Jun 18 to 20:30 on Jun 20) and Event 2 (11:00–22:00 on Oct 29), as observed in this study. Contaminants were artificially introduced using stormwater, wastewater, and well water.

4. Conclusions

- A long monitoring period (109 days) and a wide range of sensors made it possible to determine periodic water quality patterns, capture aperiodic events related to maintenance in a DWDS, and compare them to artificial contamination events on a previously unseen scale.
- The results suggest that the water quality response of contaminants can be distinguished from that of periodic fluctuations and aperiodic events with particle counters measuring particles larger than 10 μm and machine-learning-based C-particles, whereas electrochemical sensors cannot distinguish them.
- The water quality responses to aperiodic events were considerably higher than those of periodic fluctuations in particle sizes of 0.5–10 μm and in machine learning-based classes N and Small.
- The periodic pattern of the responses of particle sizes of 0.5–10 μm and particle channels N, Small, Large, B was observed as sudden spikes, which were most likely related to sudden changes in the flow rate of the building complex during working hours. Conversely, the periodic pattern of electrochemical sensors showed no such spikes, which could make the sensors/channels showing these sudden spikes more prone to false positives in EDS.
- The data analysis indicated that the periodic water quality patterns of particles were more associated with flow rate changes in the distribution system in the building complex than in those in the pressure booster station in the studied pressure zone. By contrast, the particle responses of aperiodic events found to be caused by the flow rate changes in the secondary pressure booster station.

CRediT authorship contribution statement

Markus Koppanen: Conceptualization, Methodology, Software, Validation, Formal analysis, Investigation, Resources, Data curation, Writing – original draft, Visualization, Funding acquisition. **Tero Kesti:** Conceptualization, Methodology, Software, Formal analysis, Investigation, Resources, Data curation, Visualization, Writing – original draft. **Jukka Rintala:** Writing – review & editing, Supervision, Project administration, Funding acquisition. **Marja Palmroth:** Conceptualization, Methodology, Resources, Writing – review & editing, Supervision, Project administration, Funding acquisition.

Data availability

The data that has been used is confidential.

Declaration of competing interest

Markus Koppanen reports financial support was provided by the Kaute Foundation (the Finnish Science Foundation for Economics and Technology). Markus Koppanen reports financial support was provided by the Uponor Corporation. Tero Kesti reports a relationship with the Uponor Corporation that includes: employment.

Acknowledgments

This work was supported by the Kaute Foundation (the Finnish Science Foundation for Economics and Technology) and the Uponor Corporation. We would like to thank laboratory coordinator Mika Karttunen and laboratory chief Antti Nuottajärvi at Tampere University for their practical contributions to the test environment, production engineer Sini Vuorinen and other personnel of the Tampere Water for their contribution to the data acquisition and their professional views, and CTO Markus Sunela at Fluidit Ltd. for providing us the information and his professional views on the distribution system.

Appendix A. Supplementary data

Supplementary data to this article can be found online at https://doi.org/10.1016/j.scitotenv.2023.162078.

References

Aisopou, A., Stoianov, I., Graham, N.J.D., 2012. In-pipe water quality monitoring in water supply systems under steady and unsteady state flow conditions: a quantitative assessment. Water Res. 46, 235–246. https://doi.org/10.1016/j.watres.2011.10.058.

Besmer, M.D., Sigrist, J.A., Props, R., Buysschaert, B., Mao, G., Boon, N., Hammes, F., 2017. Laboratory-scale simulation and real-time tracking of a microbial contamination event and subsequent shock-chlorination in drinking water. Front. Microbiol. 8, 1900. https://doi.org/10.3389/fmicb.2017.01900.

Besner, M.C., Prévost, M., Regli, S., 2011. Assessing the public health risk of microbial intrusion events in distribution systems: conceptual model, available data, and challenges. Water Res. 45, 961–979. https://doi.org/10.1016/j.watres.2010.10.035.

Bonett, D.G., 2006. Confidence interval for a coefficient of quartile variation. Comput. Stat. Data Anal. 50, 2953–2957. https://doi.org/10.1016/j.csda.2005.05.007.

Chen, L., Ling, F., Bakker, G., Liu, W.T., Medema, G., van der Meer, W., Liu, G., 2020. Assessing the transition effects in a drinking water distribution system caused by changing supply water quality: an indirect approach by characterizing suspended solids. Water Res. 168. https://doi.org/10.1016/j.watres.2019.115159.

Dejus, S., Neščerecka, A., Juhna, T., 2017. On-line drinking water contamination event detection methods. Vide. Tehnol. Resur. - Environ. Technol. Resour. 1, pp. 77–81. https://doi.org/10.17770/etr2017vol1.2627.

Dejus, S., Nescerecka, A., Kurcalts, G., Juhna, T., 2018. Detection of drinking water contamination event with mahalanobis distance method, using on-line monitoring sensors and manual measurement data. Water Sci. Technol. Water Supply 18, 2133–2141. https://doi.org/10.2166/ws.2018.039.

Favere, J., Buysschaert, B., Boon, N., De Gusseme, B., 2020. Online microbial fingerprinting for quality management of drinking water: full-scale event detection. Water Res. 170, 115353. https://doi.org/10.1016/j.watres.2019.115353.

Favere, J., Waegenaar, F., Boon, N., De Gusseme, B., 2021. Online microbial monitoring of drinking water: how do different techniques respond to contaminations in practice? Water Res. 202, 117387. https://doi.org/10.1016/j.watres.2021.117387.

Fish, K., Osborn, A.M., Boxall, J.B., 2017. Biofilm structures (EPS and bacterial communities) in drinking water distribution systems are conditioned by hydraulics and influence discolouration. Sci. Total Environ. 593–594, 571–580. https://doi.org/10.1016/j.scitotenv.2017.03.176.

Hofmann, H., Wickham, H., Kafadar, K., 2017. Letter-value plots: boxplots for large data. J. Comput. Graph. Stat. 26, 469–477. https://doi.org/10.1080/10618600.2017.1305277.

Højris, B., Christensen, S.C.B., Albrechtsen, H.J., Smith, C., Dahlqvist, M., 2016. A novel, optical, on-line bacteria sensor for monitoring drinking water quality. Sci. Rep. 6, 23935. https://doi.org/10.1038/srep23935.

Højris, B., Kornholt, S.N., Christensen, S.C.B., Albrechtsen, H.-J., Olesen, L.S., 2018. Detection of drinking water contamination by an optical real-time bacteria sensor. H2Open J. 1, 160–168. https://doi.org/10.2166/h2oj.2018.014.

Housh, M., Ohar, Z., 2017. Integrating physically based simulators with event detection systems: multi-site detection approach. Water Res. 110, 180–191. https://doi.org/10.1016/j.watres.2016.12.003.

Housh, M., Ohar, Z., 2018. Model-based approach for cyber-physical attack detection in water distribution systems. Water Res. 139, 132–143. https://doi.org/10.1016/j.watres.2018.03.039.

Husband, S., Boxall, J., 2016. Understanding and managing discolouration risk in trunk mains. Water Res. 107, 127–140. https://doi.org/10.1016/j.watres.2016.10.049.

Ikonen, J., Pitkänen, T., Miettinen, I.T., 2013. Suitability of optical, physical and chemical measurements for detection of changes in bacterial drinking water quality. Int. J. Environ. Res. Public Health 10, 5349–5363. https://doi.org/10.3390/ijerph10115349.

Ikonen, J., Pitkänen, T., Kosse, P., Ciszek, R., Kolehmainen, M., Miettinen, I.T., 2017. On-line detection of Escherichia coli intrusion in a pilot-scale drinking water distribution system. J. Environ. Manag. 198, 384–392. https://doi.org/10.1016/j.jenvman.2017.04.090.

Koppanen, M., Kesti, T., Kokko, M., Rintala, J., Palmroth, M., 2022. An online flow-imaging particle counter and conventional water quality sensors detect drinking water contamination in the presence of normal water quality fluctuations. Water Res. 213, 118149. https://doi.org/10.1016/j.watres.2022.118149.

Liu, G., Bakker, G.L., Li, S., Vreeburg, J.H.G., Verberk, J.Q.J.C., Medema, G.J., Liu, W.T., Van Dijk, J.C., 2014. Pyrosequencing reveals bacterial communities in unchlorinated drinking water distribution system: an integral study of bulk water, suspended solids, loose deposits, and pipe wall biofilm. Environ. Sci. Technol. 48, 5467–5476. https://doi.org/10.1021/es5009467.

Liu, S., Che, H., Smith, K., Chen, L., 2014. Contamination event detection using multiple types of conventional water quality sensors in source water. Environ. Sci. Process. Impacts 16, 2028–2038. https://doi.org/10.1039/c4em00188e.

Liu, S., Li, R., Smith, K., Che, H., 2016. Why conventional detection methods fail in identifying the existence of contamination events. Water Res. 93, 222–229. https://doi.org/10.1016/j.watres.2016.02.027.

Liu, G., Zhang, Y., Knibbe, W.J., Feng, C., Liu, W., Medema, G., van der Meer, W., 2017. Potential impacts of changing supply-water quality on drinking water distribution: a review. Water Res. 116, 135–148. https://doi.org/10.1016/j.watres.2017.03.031.

McKenna, S.A., Wilson, M., Klise, K.A., 2008. Detecting changes in water quality data. J. / Am. Water Work. Assoc. 100, 74–85. https://doi.org/10.1002/j.1551-8833.2008.tb08131.x.

McKenna, S.A., Vugrin, E.D., Hart, D.B., Aumer, R., 2013. Multivariate trajectory clustering for false positive reduction in online event detection. J. Water Resour. Plan. Manag. 139, 3–12. https://doi.org/10.1061/(ASCE)WR.1943-5452.0000240.

Mounce, S.R., Gaffney, J.W., Boult, S., Boxall, J.B., 2015. Automated data-driven approaches to evaluating and interpreting water quality time series data from water distribution systems. J. Water Resour. Plan. Manag. 141, 04015026. https://doi.org/10.1061/(asce)wr.1943-5452.0000533.

Oliker, N., Ostfeld, A., 2015. Network hydraulics inclusion in water quality event detection using multiple sensor stations data. Water Res. 80, 47–58. https://doi.org/10.1016/j.watres.2015.04.036.

Polycarpou, M.M., Uber, J.G., Wang, Z., Shang, F., Brdys, M., 2002. Feedback control of water quality. IEEE Control. Syst. Mag. 22, 68–87. https://doi.org/10.1109/MCS.2002.1004013.

Prest, E.I., Hammes, F., van Loosdrecht, M.C.M., Vrouwenvelder, J.S., 2016. Biological stability of drinking water: controlling factors, methods, and challenges. Front. Microbiol. 7. https://doi.org/10.3389/fmicb.2016.00045.

Prest, E.I., Schaap, P.G., Besmer, M.D., Hammes, F., 2021. Dynamic hydraulics in a drinking water distribution system influence suspended particles and turbidity, but not microbiology. Water (Switzerland) 13. https://doi.org/10.3390/w13010109.

Pronk, M., Goldscheider, N., Zopfi, J., 2007. Particle-size distribution as indicator for fecal bacteria contamination of drinking water from karst springs. Environ. Sci. Technol. 41, 8400–8405. https://doi.org/10.1021/es071976f.

Safford, H.R., Bischel, H.N., 2019. Flow cytometry applications in water treatment, distribution, and reuse: a review. Water Res. 151, 110–133. https://doi.org/10.1016/j.watres.2018.12.016.

Sorensen, J.P.R., Baker, A., Cumberland, S.A., Lapworth, D.J., MacDonald, A.M., Pedley, S., Taylor, R.G., Ward, J.S.T., 2018. Real-time detection of faecally contaminated drinking water with tryptophan-like fluorescence: defining threshold values. Sci. Total Environ. 622–623, 1250–1257. https://doi.org/10.1016/j.scitotenv.2017.11.162.

Sorensen, J.P.R., Vivanco, A., Ascott, M.J., Gooddy, D.C., Lapworth, D.J., Read, D.S., Rushworth, C.M., Bucknall, J., Herbert, K., Karapanos, I., Gumm, L.P., Taylor, R.G., 2018. Online fluorescence spectroscopy for the real-time evaluation of the microbial quality of drinking water. Water Res. 137, 301–309. https://doi.org/10.1016/j.watres.2018.03.001.

Stedmon, C.A., Seredyńska-Sobecka, B., Boe-Hansen, R., Le Tallec, N., Waul, C.K., Arvin, E., 2011. A potential approach for monitoring drinking water quality from groundwater systems using organic matter fluorescence as an early warning for contamination events. Water Res. 45, 6030–6038. https://doi.org/10.1016/j.watres.2011.08.066.

Storey, M.V., van der Gaag, B., Burns, B.P., 2011. Advances in on-line drinking water quality monitoring and early warning systems. Water Res. 45, 741–747. https://doi.org/10.1016/j.watres.2010.08.049.

Sunny, I., Husband, P.S., Boxall, J.B., 2020. Impact of hydraulic interventions on chronic and acute material loading and discolouration risk in drinking water distribution systems. Water Res. 169, 115224. https://doi.org/10.1016/j.watres.2019.115224.

Verberk, J.Q.J.C., Hamilton, L.A., O'Halloran, K.J., Van Der Horst, W., Vreeburg, J., 2006. Analysis of particle numbers, size and composition in drinking water transportation pipelines: results of online measurements. Water Sci. Technol. Water Supply 6, 35–43. https://doi.org/10.2166/ws.2006.902.

Vreeburg, J.H.G., Schippers, D., Verberk, J.Q.J.C., van Dijk, J.C., 2008. Impact of particles on sediment accumulation in a drinking water distribution system. Water Res. 42, 4233–4242. https://doi.org/10.1016/j.watres.2008.05.024.

Waskom, M., 2021. Seaborn: statistical data visualization. J. Open Source Softw. 6, 3021. https://doi.org/10.21105/joss.03021.